Revolutionizing Brain Tumor Segmentation in MRI with Dynamic Fusion of Handcrafted Features and Global Pathway-based Deep Learning

Faizan Ullah[1], Muhammad Nadeem[1], and Mohammad Abrar[2,3,*]
[1] Department of Computer Science, International Islamic University, Islamabad, 44000, Pakistan
[e-mail: faizan.phdcs157, nadeem@iiu.edu.pk]
[2] Faculty of Computer Studies, Arab Open University, Muscat, 130, Sultanate of Oman
[e-mail: abrar.m@aour.edu.om]
[3] Department of Computer Science, Bacha Khan University, Charsadda, 24420, Pakistan
[*]Corresponding author: Mohammad Abrar

Received May 29, 2023; revised September 27, 2023; accepted October 6, 2023; published January 31, 2024

Abstract

Gliomas are the most common malignant brain tumor and cause the most deaths. Manual brain tumor segmentation is expensive, time-consuming, error-prone, and dependent on the radiologist's expertise and experience. Manual brain tumor segmentation outcomes by different radiologists for the same patient may differ. Thus, more robust, and dependable methods are needed. Medical imaging researchers produced numerous semi-automatic and fully automatic brain tumor segmentation algorithms using ML pipelines and accurate (handcrafted feature-based, etc.) or data-driven strategies. Current methods use CNN or handmade features such symmetry analysis, alignment-based features analysis, or textural qualities. CNN approaches provide unsupervised features, while manual features model domain knowledge. Cascaded algorithms may outperform feature-based or data-driven like CNN methods. A revolutionary cascaded strategy is presented that intelligently supplies CNN with past information from handmade feature-based ML algorithms. Each patient receives manual ground truth and four MRI modalities (T1, T1c, T2, and FLAIR). Handcrafted characteristics and deep learning are used to segment brain tumors in a Global Convolutional Neural Network (GCNN). The proposed GCNN architecture with two parallel CNNs, CSPathways CNN (CSPCNN) and MRI Pathways CNN (MRIPCNN), segmented BraTS brain tumors with high accuracy. The proposed model achieved a Dice score of 87% higher than the state of the art. This research could improve brain tumor segmentation, helping clinicians diagnose and treat patients.

Keywords: Brain tumor, Health Risks, Handcrafted features, Global-pathway CNN, Local-pathway CNN.

http://doi.org/10.3837/tiis.2024.01.007 **ISSN : 1976-7277**

1. Introduction

The brain is one of the most intricate and complicated organs in the human body. Humans encounter numerous diseases in their lifetime. Sometimes these diseases get worse and resultantly human lives are lost. Therefore, researchers in the medical field are trying their best to tackle these diseases well in time. Timely and accurate diagnosis plays a vital role in the prevention of such fatal diseases [1]. Brain Tumors (BT) are continuously posing threats to humanity. Brain tumors are irregularly growing tissue that results from uncontrolled cell reproduction. It has no physiological function within the neuro system of the human body. Tumors produce swelling, increase size, and exert pressure on the brain. It results in the appearance of some abnormal neurological symptoms in the patient. Frequent headaches and migraines could be some of the signs of malignancy. It could also result in eyesight loss [2] . American Brain Tumor Association (ABTA) stated brain tumors as [3] enhancing tumors.

- Cancer ranks second among the leading causes of death among children younger than 20.
- In males between the ages of 20-39 cancer is the second major cause of death.
- Cancer is the seventh biggest cause of mortality among 20-39-year-old females.
- The number of young people in their adolescence and young adulthood diagnosed with a primary brain tumor in 2021 was estimated to be around 11,700.
- In 2021, over three thousand children were diagnosed with a primary brain tumor.
- According to a report conducted from 2013-to 2017, at the age of 40+ brain tumors were reported as the 3rd most common cause of cancer deaths.

Globally cancer is considered as the second major cause of death. Low-income to middle-income nations are the most affected from the deadly disease contributing around 70 percent of the total. As for 630 000 reported cases identified each year and 350 000 deaths, neck and head malignancies are the sixth most frequent malignancy globally. It is a major cause of cancer-related death worldwide, with an annual number of 4–5 per 100,000 cases, accounting for 2% of all cancer fatalities. Every year, 1, 50,000 new cancer cases are diagnosed in Pakistan, with 60–80 percent of cancer patients dying [4].

Medical professionals employ a range of methods for the detection of brain tumors X-rays, Position Emission Tomography (PET), Computed Tomography (CT), and MRI are among the modalities that are frequently used [5]. MRI can better help doctors when other imaging techniques are unable to provide enough clues in complicated cases. An MRI scan creates a realistic representation by combining the characteristics of magnetism and radio waves [6]. MRI offers functional and anatomical information, has better soft tissue resolution, doesn't involve ionizing radiation, and doesn't call for radioactive tracers, MRI is preferred over CT and PET scans for the detection of brain tumors. MRI has emerged as the prime imaging modality in radiology owing to its non-invasive characteristics, enabling clinicians to examine the internal structure of the brain [7]. MRIs provide enough information even to detect the tiniest anomalies. However, the advancement in computational technology is attracting clinicians in early detection of tumors in the brain.

The primary purpose of computer-based brain tumor diagnosis is to acquire crucial clinical information on the existence, location, and type of tumor [8].

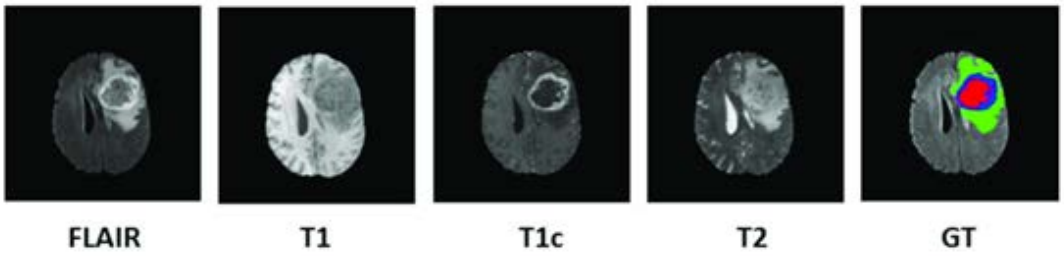

Fig. 1. MRI scans of BraTS Dataset

MRI imaging is used to segment brain tumors. To construct a 3D image of the brain, medical professionals use four distinct MRI weighted modalities, namely T1-weighted, T1-contrast weighted, T2-weighted, and FLAIR. BT can be divided into four subtypes [9]. i.e., active tumorous tissues, narcotic tissues, and edema as shown in **Fig. 1**.

Image Segmentation basically partitions a digitized image into subsets of pixels known as image objects, which could also lessen the image's dimensionality and make studying it easier [10].

Semantic image segmentation predicts a class label in an input image at each pixel level [11]. It defines objects within a given image. Image segmentation is considered as a fundamental part of image analysis in medical applications. Image analysis along with classification and abnormality detection is in practice by the majority of radiologist worldwide [12]. The term "image segmentation" refers to the process of locating components and edges in images. The shape of cancerous cells plays a vital role in determining the severity of the illness. In this context, object recognition might not prove helpful, even with all the components combined. It would only result in creating bounding boxes, which would not aid in identifying the cellular structure. In segmentation process, first is to locate the tumor zone, followed by the identification of the healthy and unhealthy zones. Then segmentation of the sub-regions takes place. The study introduces a novel approach for segmenting brain tumors, which involves a cascaded methodology that merges handcrafted features with Deep CNN. The proposed framework includes a Confidence Surface (CS) pathway CNN and an MRI pathway CNN. The handcrafted features, which capture domain knowledge, are computed in a local neighborhood at each pixel location and then concatenated to generate a single feature vector. The CS pathway CNN processes the output of handcrafted features, and the MRI pathway CNN processes the four MRI modalities along with the provided ground truth. The proposed global CNN architecture achieved high accuracy in brain tumor segmentation. However, the use of a limited dataset and the requirement of expert knowledge to generate handcrafted features may limit the generalizability of the proposed framework. The effectiveness of segmentation on larger datasets could be enhanced in the future by integrating different types of handcrafted features and exploring the possibility of transfer learning.

The paper is organized into several sections. In Section 2, an overview of relevant literature on handcrafted and cascaded approaches is presented. Section 3 describes the proposed model, while Section 4 details the dataset and experimental setup. Finally, in Section 5, the paper concludes with some closing remarks and potential avenues for future research.

2. Related work

Generally, detecting brain tumor in MRI images takes place after a detailed analysis by the radiologist. This analysis takes sufficiently longer time. The main motive is to design a

comprehensive tool which could be used as a second opinion by the radiologist.

2.1 Handcrafted features

A variety of techniques have been used in the literature for feature extraction. Two broader categories of feature extraction namely global and local have been discussed by the research community in the computer vision and image processing domain.
The global feature sets consist of traits and intensity, first-order statistics (for example, mean, skewness, and standard deviation), and second-order statistics (such as Gabor features, wavelet transform (WT), Gray-Level Co-occurrence Matrix (GLCM), and structural elements) [13].
For tumor recognition and classification [14],They utilized discrete wavelet transformation-based and GLCM based approaches. Low-level features conveniently depict the image; yet, because most gliomas have identical texture, border, form, and volume, low-level features, and their representational ability are restricted. [15] used DWT to get the features and detailed coefficient level-3 decomposition is used. Moreover, Color Moments (CM) to minimize the coefficient. Subsequently, the output is fed forward into an ANN to differentiate between normal and pathological brain MR images.

The local feature is the second sort of feature. The extraction of local features is also crucial in the detection of brain tumors. Fisher vector (FV), scale-invariant feature transformation (SIFT), and bag-of-words (BoW) are examples of local features. BoW has been used by a community of scholars for medical picture retrieval and categorization. For example, in mammography, the classification of breast tissue density [16] , Retrieval and categorization of X-ray pictures at the pathology and organ levels [17], as well as content-based retrieval of brain tumors. Cheng *et al*, [18] utilize local based statistical features SIFT, FV, and BoW to extract tumor area from brain. The summarized comparison is presented in **Table 1**.

Table 1. Comparative Analysis of Feature Extraction Techniques

Ref	Year	Technique used	Features	Classifier	Limitation
[14]	2012	GLCM, DWT	Global Features	Probabilistic Neural Network (PNN)	A limited no of the feature set is fed to classifiers. Using only two types of features results in low accuracy.
[18]	2016	FV, SIFT, BoW,	Local Features	Content based image retrieval	High dimension features are used which makes the proposed system computationally expensive
[16]	2018	LBP	Local Features	CNN	Classification of breast tissue density in mammogram
[13]	2020	GLCM, WT, Gabor feature,	Global Features	KNN, LSTM	May ignore more important features as such techniques do not use pixel-level information
[15]	2020	3 level DWT, Color Shape, mean, standard deviation	Global Features	CNN	Local-level information is ignored which impacts results negatively.

2.2 Cascaded Approach for Tumor Segmentation

In recent years, segmentation of brain tumor regions has garnered considerable interest. Numerous studies have developed diverse techniques for segmenting and classifying tumor regions on MRI imaging. This increasing interest highlights the significance of developing automated tools for the segmentation of brain tumors [19].

Deep learning approaches, notably CNNs, have been used for a range of computer vision problems with state-of-the-art outcomes. Image classification [20], object recognition [21]and biomedical image segmentation [12] are just a few examples. CNN has the potential to understand in a hierarchical order of progressively complicated features directly from data. This is accomplished by using a convolutional layer's result feature maps as input channels for the next convolutional layer. This distinct property has not only made CNN the first option that many biomedical image researchers attempted on brain tumor segmentation brain task to investigate its segmentation accuracy but also stated, that research that employed CNN based model primarily concentrates on designing networks rather than following the traditional ML pipeline (i.e., image preprocessing, features selection, feature extraction, dimensionality reduction and finally training classifier). In this regard, different researchers proposed distinct CNN architectures and processed the MRI modalities in distinct fashions (i.e. either 2D patches based or 3D patches based) and obtained competitive segmentation results [22].

Proposed cascaded CNN [23] based on two paths to segments sub-region of brain tumor. Three types of handcrafted features are extracted and SVM is utilized to perform classification. The author achieves a dice similarity score of 0.76 on core, 0.81 on a complete, and 0.73 on enhancing tumor, respectively. As discussed above, the authors have used two-path CNN with the same input and kernel size for both global and local pathways. A small kernel dimension is used in global pathways that affect the segmentation results.

Kleesiek *et al.* [24]presented a 3D-CNN framework. A CNN is fed with 3D patches or voxel cubes derived from different brain MRI slices. The model then predicts the label of the tissue located at the center of each cube. They reported an average score of 0.87 for the entire tumor region, whereas the score was for the active tumor region at 0.73 for the BraTS dataset. Even though the suggested network produced favorable performance among three tumors, the network computational overhead was higher due to the CNN (i.e., 3D-CNN) based on 3D patches compared to 2D patches-based approaches. Only one type of feature is considered which provides insufficient information. Only local features are extracted, and global features are ignored which is most important for segmentation.

Zikic *et al.* [25] developed a 2D patch-based 2D-CNN architecture. This model can perform tumor segmentation. It lightens the computational burden on the system. The research reported a dice score for the overall tumor region as 0.83 and 0.736 for the core tumor region. For the active tumor region in the BraTS dataset the score stood at 0.69. A shallow CNN is introduced with a small patch size is introduced which recognizes brain tumor segments.

The authors have utilized a small patch size, which is not good for extracting global features. The proposed system uses a non-overlapping Max pooling layer. There is a high chance it will miss key features. By identifying different sized patches at the same time, Havaei *et al.* [26] proposed CNN architecture consists of two pathways. It works in sequence to analyze local and global features of brain MRI data. In this work each pathway takes patches from separate MRI modalities, with the local pathway using 33 × 33 pixel patches and the global pathway using 65 × 65 pixel patches. Both pathways are centered at the same location to identify the label of the central pixel. The results on the BraTS dataset were satisfactory, with an overall accuracy of 0.88 for the entire tumor region, 0.79 for the core tumor region, and 0.73 for the active tumor region. The authors have applied two pathway CNN in applied with a smaller

number of layers and a large kernel size is applied. Large kernel size causes high computational cost.

The brain tumor was divided into three categories by Wang *et al.* [15]. The authors suggested a method for complete tumor, core tumor, and full tumor that uses two different CNNs. The first network is used to segment the entire tumor, and its output's bounding box is then utilized as the input for the second network to segment the main tumor. The second network operates on a subset of the first network's output to achieve a more refined segmentation of the core and complete tumor. The process involves segmenting the enhancing tumor through utilization of the bounding box derived from the core tumor segmentation outcomes.

Due to the involvement of a high set of variables in three CNNs, this approach works well but is computationally costly. Local features, on the other hand, were only concentrated on its strategy via smaller size convolutional kernels. Furthermore, during the testing phase, researchers employed data augmentation, which doubled the processing time of their suggested technique.

Savadikar *et al.* [27] proposed segmentation solution for BraTS challenge.. The study employed Probabilistic UNet to see how sampling alternative segmentation maps and 2D segmentation models affected the results. Self-attention is employed in the Unet, as well as the prior and posterior systems, to guarantee the consistency of suggested models, and to investigate the impact of raising the number of concentration blocks on the quality of segmentation. They reported a Dice score of 0.81898 for the whole tumor. For the tumor core the score was 0.71681, while a score of 0.68893 was reported for enhancing tumor.

Kayalibay *et al.* [28] used a CNN-based algorithm with a three-dimensional kernel The authors evaluated BraTS 2013 and 2015 datasets and achieved dice scores 0.87 for the overall tumor region, 0.74 for the core tumor region, and 0.71 for the active tumor region. Similarly, for the whole tumor region, the dice score was 0.85, for the core tumor region it was 0.72, and for the active tumor region it was 0.61.

Iqbal *et al.* [29] in an article demonstrated that how to segment brain tumors in MRIs using a deep CNN. The presented system was based on the BraTS segmentation challenge dataset, consisting of images collected via four distinct modalities. As a result, the investigators provide an advanced form of a current network to tackle the issues of segmentation. The network architecture involves the sequential connection of several layers of neural networks, wherein Convolutional feature maps are supplied at the peer level. The suggested approach's usability and superiority over previous methods in this field of research are demonstrated by experimental findings using BraTS 2015 benchmark data. The summarized comparison in shown in **Table 2** below:

Table 2. State-of-the-art CNN based Methods for Tumor Segmentation and Grading.

Ref	Method	Dataset	Performance Measure (Dice Score)			Year
			Whole tumor	Core tumor	Active tumor	
[24]	3D-CNN using 3D. convolutional filters	BraTS	0.87	0.77	0.73	2014
[25]	Slice wise 2D-patches are extracted. 2D-CNN	BraTS	0.83	0.73	0.69	2014
[28]	3D-patches are extracted using 3D-CNN	BraTS	0.86	0.74	0.71	2017

Ref	Method	Dataset	Performance Measure (Dice Score)			Year
			Whole tumor	Core tumor	Active tumor	
[26]	2DCNN patch based two cascaded pathways (Local and Global)	BraTS	0.86	0.79	0.73	2017
[29]	Extracted multi 2D patches using pixel level different CNN layers.	BraTS	0.67	Not ported	Not reported	2018
[15]	Two different CNNs for segmentation and detection	BraTS	0.89	0.83	0.78	2019
[23]	2D-CNNs	BraTS	0.76	0.81	0.73	2020

3. Methodology

This section highlights the research methodology of the proposed extended handcrafted feature-based ML technique for Brain tumor segmentation using multiple MRI pathways. The Dice Similarity Score (DSS) as an assessment metric was utilized to evaluate the effectiveness of the proposed approach. This methodology consists of handcrafted feature extraction, feature labeling, confidence surface generation, and acquisition of the dataset. A new cascaded approach for fully automated brain tumor segmentation is developed that first customizes HGG and LGG in MRI images. Then the results of HGG and LGG are fed as input to Deep Neural Networks in the form of previous information. Due to significant variation in the presence, absence, density, contrast and the location of tumor, the embedding of prior knowledge is challenging in the brain tumor segmentation as compared to other similar medical tasks.

3.1 Hand Crafted Feature Extraction

Different handcrafted features were calculated like Extended Local Binary Pattern (ELBP), DWT, and GLCM.

3.1.1 Extended Local Binary Pattern

Local Binary Pattern (LBP) is a robust non-parametric method for feature extraction. This technique extracts comparatively accurate features with high accuracy and reasonable processing time. It applies a 3 × 3 mask to extract the grayscale value of the middle pixel. **Fig. 2** depicts the prime idea of this work.

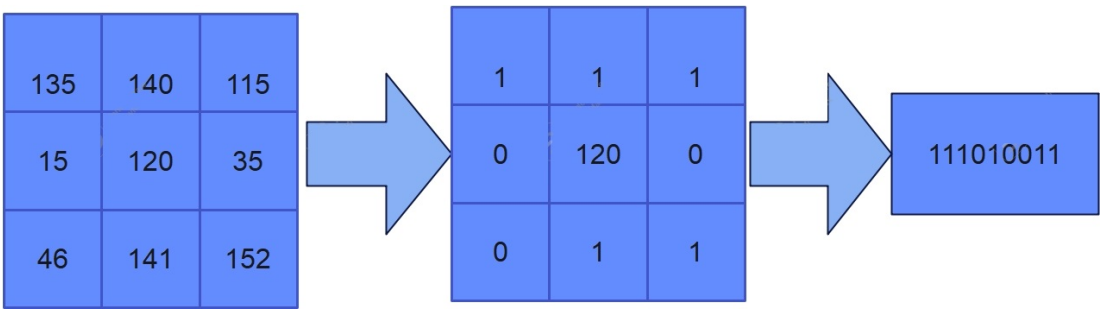

Fig. 2. An Overview of Feature Extraction Process of LBP

In this process, it calculates the middle pixel with the neighbor pixels to convert the numeric value to binary. If the value of the neighbor pixel is greater, assign them with the value 1, else 0. Finally, the decimal value is calculated from extracted 1's and 0's to obtain the LBP operator of the middle value. This procedure is repeated for every image by shifting the mask in each individual image. This process is computationally inexpensive and produces more accurate results. However, the LBP cannot completely display the structure of the image. Similarly, it cannot contain all the spatial information. The LBP uses scaling, recurrence, and introduction as coding for every pixel. In this way, it compromises precision. To address these issues, Extended Local Binary Pattern (ELBP) was used as shown in **Algorithm 1**. ELBP is an enhanced algorithm that uses scaling, recurrence, and introduction as a coding scheme in a parallel manner. Thus, it improves the performance of LBP by using parallelism and increases the precision by concurrently using these coding schemes. The resultant algorithm enhances the arrangement exactness of the proposed brain tumor location framework.

Algorithm 1: Extended Local Binary Pattern

```
Begin ELBP
        Get preprocessed MRI(IMG)
        for X to range (0, length (IMG))
                for Y in range (0, length (IMG))
                        Get center IMG [X][Y]
                        IMG(length-1)*249+1= LBP(Val)
                        Val++;
                        for i=0 range 511 til 64
                                for j=0 range 511 til 64
                                        Ex= BI(i:1 to 63 p;p to 63)
                                         IMG(( length x=1)* 256 +1)(length y-1)*256
                                         +1)) = ELBP( Val)
                                        // sum of generated features
                                end j
                        end i
                End Y
        End X
End ELBP
```

3.1.2 Discrete Wavelet Transformation

The DWT is employed to break down the input brain MRI image into various sub-bands. These sub-bands comprise an approximation sub-band isolating low-frequency data, along with diagonal, vertical, and horizontal sub-bands. In the initial decomposition stage, the input brain

MRI image is split into four sub-bands: LL (Low-Low approximation), LH (Low-High horizontal), HL (High-Low vertical), and HH (High-High diagonal). During the second level of decomposition, DWT is applied over the LL sub-band, which further generates HH2, HL2, LH2, and LL2. While, at third level DWT transformation, LL2 is decomposed into four bands to produce third level sub bands HH3, HL3, LH3, and LL3. Furthermore, fourth level DWT decomposition is applied over LL3. A four-level decomposition was applied to the brain MRI images, and the resulting extracted features were used to classify them as either malignant or benign.

$$\varphi(x)=\sum_{k=-\infty}^{\infty} ak\varphi(sx-k) \quad (1)$$

$$\int_{-\infty}^{\infty} \varphi(x)\varphi(x+1)dx = \delta 0, l \quad (2)$$

$$x = \sum_{=-\infty}^{\infty}(1)]^k\ [aN-1-k(2x-k)] \quad (3)$$

Fig. 3 displays the sub-band images obtained from applying the DWT to the brain MR images at a four-level decomposition.

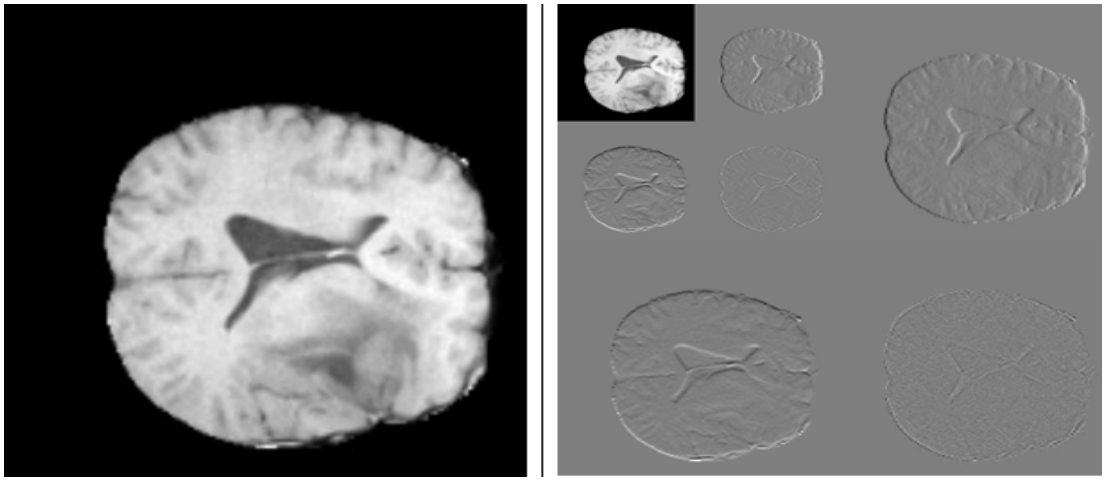

Fig. 3. A Decomposition of Brain MRI Images using DWT at level 4

3.1.3 GLCM Features

GLCM is a statistical approach for feature extraction. GCLM features map is produced using pixels' orientations at 00, 450, 900, and 1350. The pixel orientation at 450 is used for constructing the matrices. The process is presented in Equation 4 and Equation 5, the Gray Level Co-occurrence Matrix (GLCM) is a matrix where P(i, j) represents the number of times the ith pixel with value i occurs in a specific orientation 450 and is adjacent to the jth pixel with value j. From this matrix, relevant features such as correlation, contrast, entropy, and energy are extracted for use in the classification of brain MRI.

$$contracCM = \sum_{j,i-1}^{m} P(i,j) * [(i-j)]2 \quad (4)$$

$$CorrelationGM = \frac{\sum_{J,1=1}^{m} P(i-\mu i)*(i-\mu\, j)2*P(i,j)}{\sigma J \sigma i} \quad (5)$$

In this context, $\mu\iota$ and μj represent the means of the GLCM matrix in the x and y directions, respectively, while N denotes the number of rows and columns in the GLCM matrix. When calculating GLCM-based features, σi and σj stand for the standard deviations of the GLCM matrix in the x and y directions, respectively.

3.2 Feature Labeling

In this phase, features were labeled against the provided ground truth. **Fig. 4** illustrate the feature labeling process.

Fig. 4. An Illustration of the Proposed Feature Labelling Process.

3.3 Confidence Surface Generation

Finally, the generated feature vectors are mapped as additional MRI modality. Which is named Confidence Surface (CS) shown in **Fig. 5**.

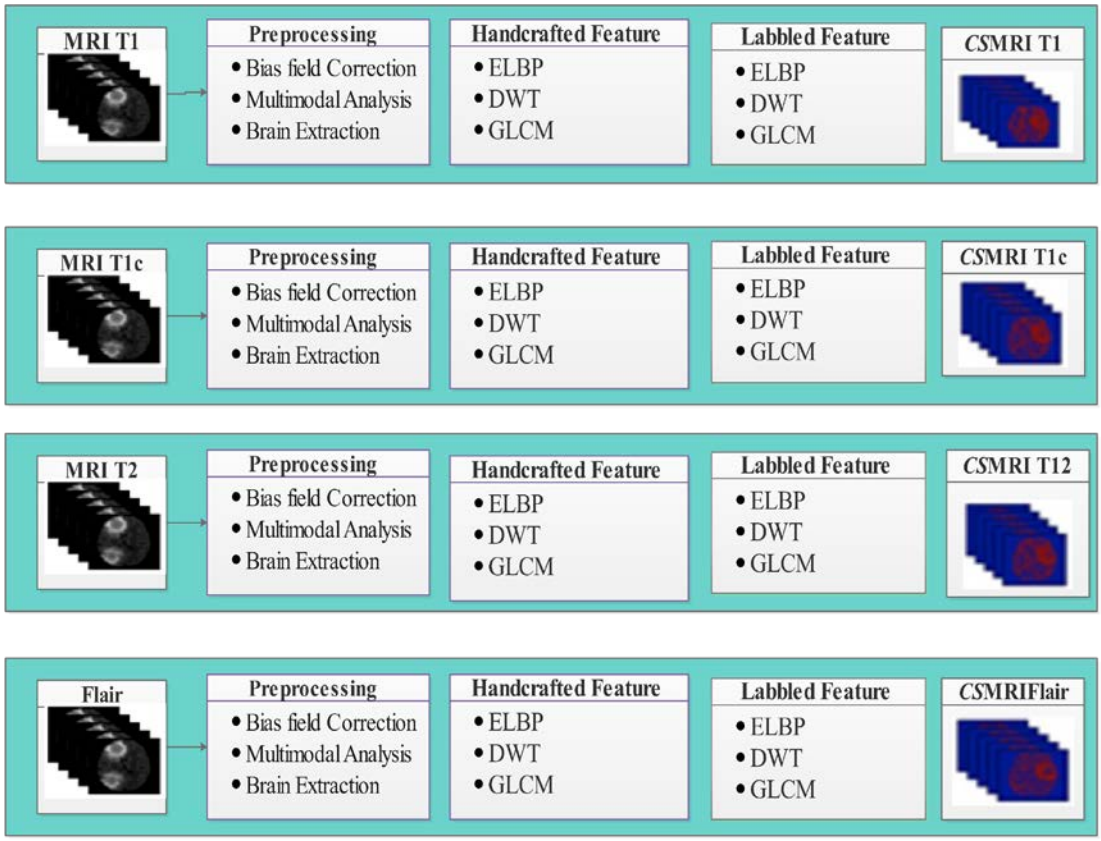

Fig. 5. An Illustration of the Confidence Surface Generation Process.

3.4 Dataset

The Brain Tumor Segmentation (BraTS) [30] challenge investigates methodologies for segmenting brain tumors, with a focus on Gliomas, which represent the most widespread primary brain neoplasms. The dataset is composed of MRI volumes measuring 240x240x155, showcasing four varying contrast modalities: T1, T1c, T2, and FLAIR. Each voxel is annotated with one of five tumor sub-region labels, including necrosis (NCR), edema (ED), non-enhancing tumor (NET), enhancing/active tumor (AT), and all other classifications. The BraTS 2018 dataset encompasses 210 high-grade gliomas (HGG) and 75 low-grade gliomas (LGG) MRI examinations.

3.5 Data Augmentation

BraTS benchmark dataset was used for, and it consists of a small number of images. On the contrary, CNN requires a high number of training samples to learn high dimension features. Otherwise, there is a high risk of overfitting. To reduce the risk of overfitting, many authors have used data augmentation techniques [31]. Data augmentation increases the number of samples by taking copies using flipping, rotation, and mirroring dimensions. A combination of these data augmentation techniques for increasing the training samples was adopted in the study.

3.6 CNN Architecture

After the successful generation of the CSmodalities with handcrafted features, the proposed-global CNN (GCNN) architecture is comprised of two parallel CNNs. Each CNN uses two pathways (i.e., local, and global pathways) shown in **Fig. 6**.

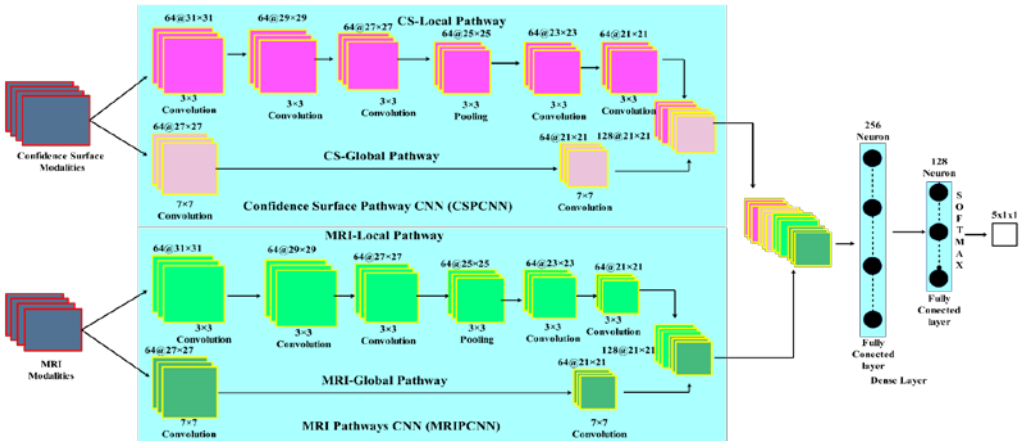

Fig. 6. The Proposed GCNN Architecture

First CNN is called CSPCNN. The CSmodalities along with the given manual ground truth is processed. The second CNN is called MRI Pathways CNN (MRIPCNN). Along with the provided manual ground truth, the MRI modalities are processed. The local pathways of both CSPCNN and MRIPCNN consist of five convolutional layers with a convolutional kernel of size 3×3 at stride 1 and one pooling layer with kernel size 3×3 at stride 1, 3,4, and 5. Shown in **Table 3** and **Table 5**.

Table 3. Architectural detail of CSPCNN Local Pathway

Layer	Type	Filter size	Strides	Filters	FC unit	Input	Output
Layer1	Convolution	3×3	1×1	64	-	4×33×33	64×31×31
Layer2	Convolution	3×3	1×1	64	-	64×31×31	64×29×29
Layer3	Convolution	3×3	1×1	64	-	64×29×29	64×27×27
Layer4	Max-pool	3×3	1×1	-	-	64×27×27	64×25×25
Layer5	Convolution	3×3	1×1	64	-	64×25×25	64×23×23
Layer6	Convolution	3×3	1×1	64	-	64×23×23	64×21×21

Table 4. Architectural detail of CSPCNN global Pathway

Layer	Type	Filter size	Strides	Filters	FC unit	Input	Output
Layer1	Convolution	7×7	1×1	128	-	4×33×33	128×27×27
Layer2	Convolution	7×7	1×1	128	-	128 × 27×27	128×21×21

Table 5. Architectural detail of MRIPCNN Local Pathway

Layer	Type	Filter size	Strides	Filters	FC unit	Input	Output
Layer1	Convolution	3×3	1×1	64	-	4×33×33	64×31×31
Layer2	Convolution	3×3	1×1	64	-	64×31×31	64×29×29
Layer3	Convolution	3×3	1×1	64	-	64×29×29	64×27×27
Layer4	Max-pool	3×3	1×1	-	-	64×27×27	64×25×25
Layer5	Convolution	3×3	1×1	64	-	64×25×25	64×23×23
Layer6	Convolution	3×3	1×1	64	-	64×23×23	64×21×21

First CNN is called CSPCNN. The CSmodalities along with the given manual ground truth is processed. The second CNN is called MRIPCNN. The MRI modalities along with the given manual ground truth is processed. The local pathways of both CSPCNN and MRIPCNN consist of five convolutional layers with a convolutional kernel of size 3×3 at stride 1 and one pooling layer with kernel size 3×3 at stride 1, 3, 4, and 5.
Similarly, the global pathways of both CSPCNN and MRIPCNN are comprised of two convolution layers with convolutional kernels of size 7×7 at stride 1 see in **Table 4** and **Table 6**.

Table 6. Architectural detail of CSPCNN Global Pathway

Layer	Type	Filter size	Strides	Filters	FC unit	Input	Output
Layer1	Convolution	7×7	1×1	128	-	4×33×33	128×27×27
Layer2	Convolution	7×7	1×1	128	-	128×27×27	128×21×21

Table 7. Architectural detail of Global CNN

Type	Filter size	Strides	Filters	FC unit	Input	Output
FC	256				256 × 21 × 21	14,450,688
FC	128				-	
SoftMax	5				-	

The architectures of the two CNNs are integrated by merging their respective feature maps show in **Table 7**. Subsequently, the amalgamated feature maps are processed through two densely connected layers. The ultimate segmentation is executed utilizing SoftMax activation. The ReLU function is used to estimate the performance of the model.

4. Experiments

The overall research implementation process is split into two stages. The first stage contains the implementation of the handcrafted features (i.e., ELBP, DWT, and GLCM) at each pixel neighborhood. The second phase consists of the implementation of GCNN (i.e., CSPCNN and MRIPCNN).

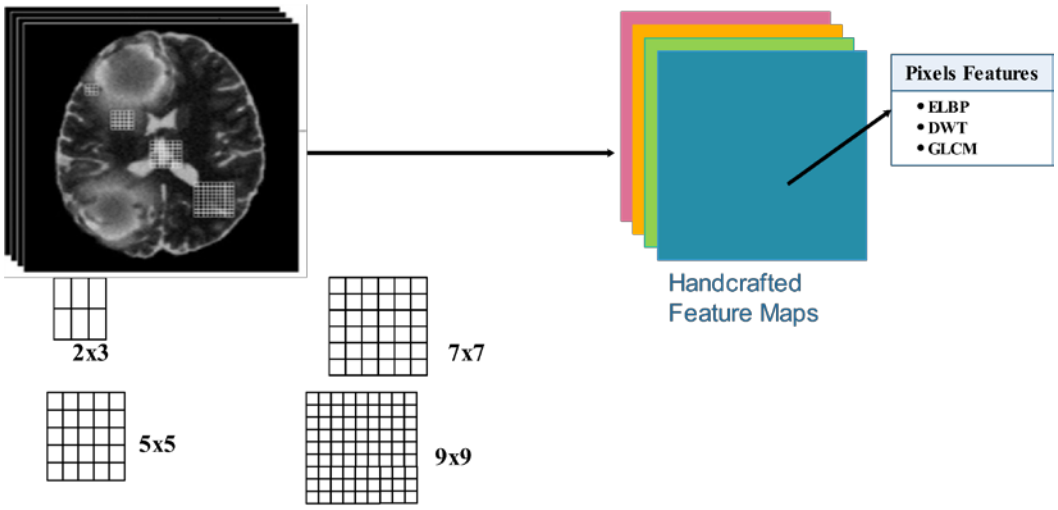

Fig. 7. Pixel Level Neighborhood with Kernel Sizes of 3,5,7, and 9

In the phase, three handcrafted features i.e., ELBP, DWT, GCLM are computed in a local neighborhood at each pixel location shown in **Fig. 7**.
The computed features are merged to build a single feature vector and then label each pixel as either healthy or tumorous **Fig. 8**.

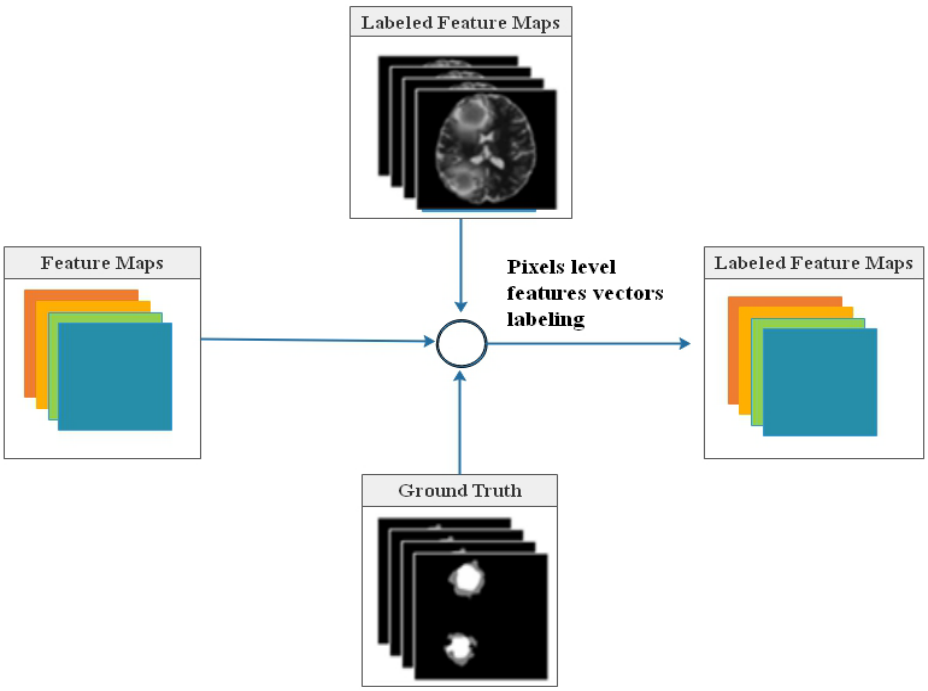

Fig. 8. Labeling Process at Pixel Level

In the dataset, each MRI modality is assigned a unique contrast signature to the same tumor pixel location. Taking inspiration from this observation a separate modality has been created from handcrafted features.
This pixel classification generates four CSmodalities shown in **Fig. 9, 10, 11, 12**. Three horizontal and vertical strides in the healthy region and one horizontal and vertical stride in the tumor region were adopted. Due to the class imbalance issue, the results of handcrafted techniques are positively biased. This results in better quality CSmodalities, which is directly affecting ultimate brain tumor segmentation. The output of the first phase (i.e., CSmodalities) is supplied as an input to CSPCNN during the second phase of implementation. CSPCNN processes the output of handcrafted features, based on traditional ML, which ultimately act as estimated prior knowledge in GCNN.

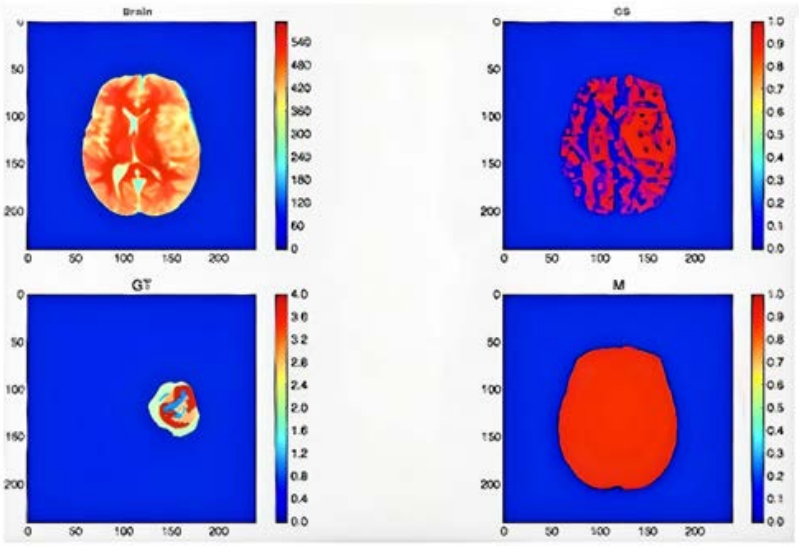

Fig. 9. T1-weighted MRI confidence surface

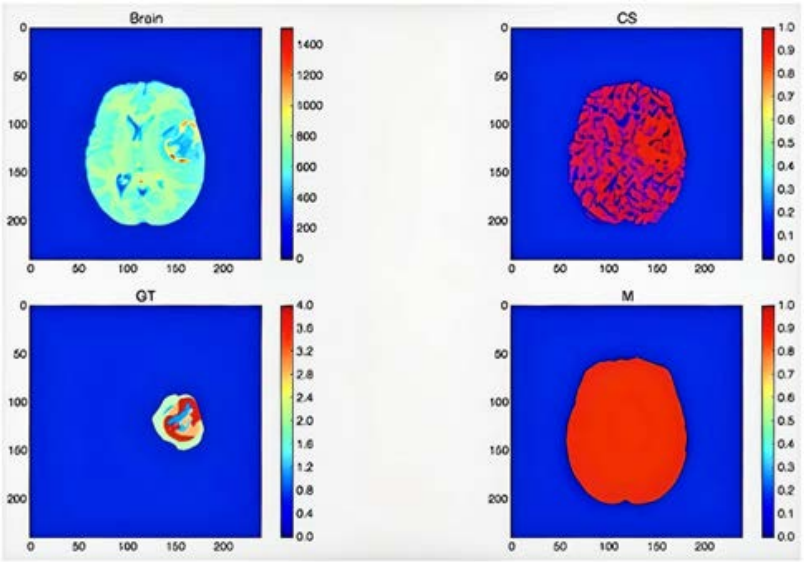

Fig. 10. T1c-weighted MRI confidence surface

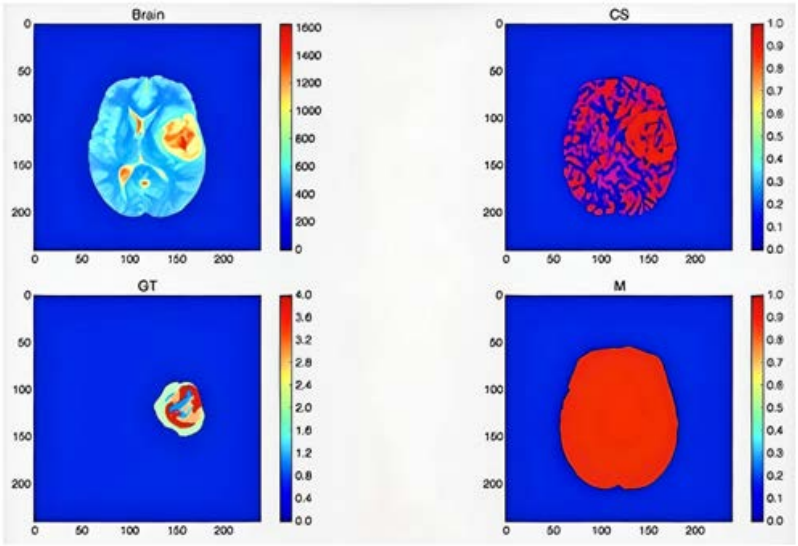

Fig. 11. T2-weighted MRI confidence surface.

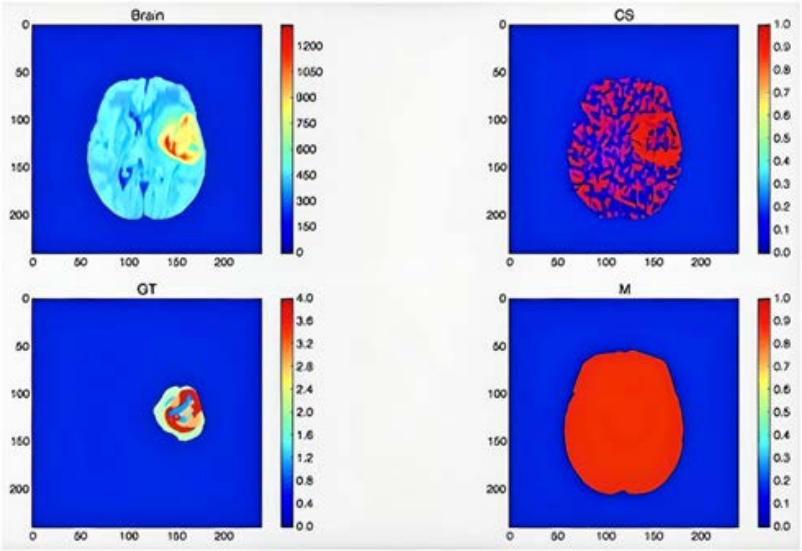

Fig. 12. FLAIR MRI confidence surface

During the second phase of the implementation process, the output of the first phase (i.e., CS-modalities) along with the given ground truth is provided to CSPCNN as input. Similarly, four MRImodalities (i.e., T1, T1c, T2, FLAIR) along with ground truth is also provided to MRIPCNN as input. The detailed information on CSPCNN, MRIPCNN, and GCNN can be seen in **Fig. 8**. To evaluate the efficacy of the proposed model, a thorough analysis was conducted employing various widely accepted metrics such as accuracy, precision, recall, and F1-score.

The training loss **Fig. 13** illustrates the gradual decrease in loss throughout the training process. This reduction in loss signifies that the model is effectively learning and improving its predictive capabilities as it iterates over the training data.

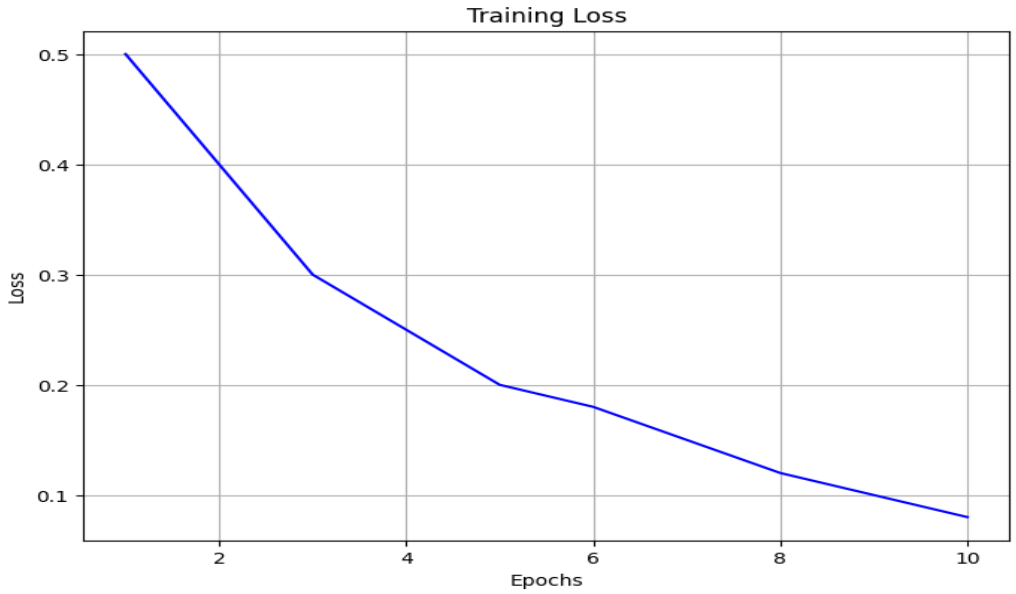

Fig. 13. Training Loss of the Proposed Model

The validation loss **Fig. 14** presents the loss on an independent validation dataset, offering valuable insights into the model's generalization to unseen data. An ideal scenario is for the validation loss to exhibit a similar trend to the training loss, indicating that the model is not overfitting. These figures depicting the loss functions provide a visual representation of the convergence and optimization performance of the proposed model.

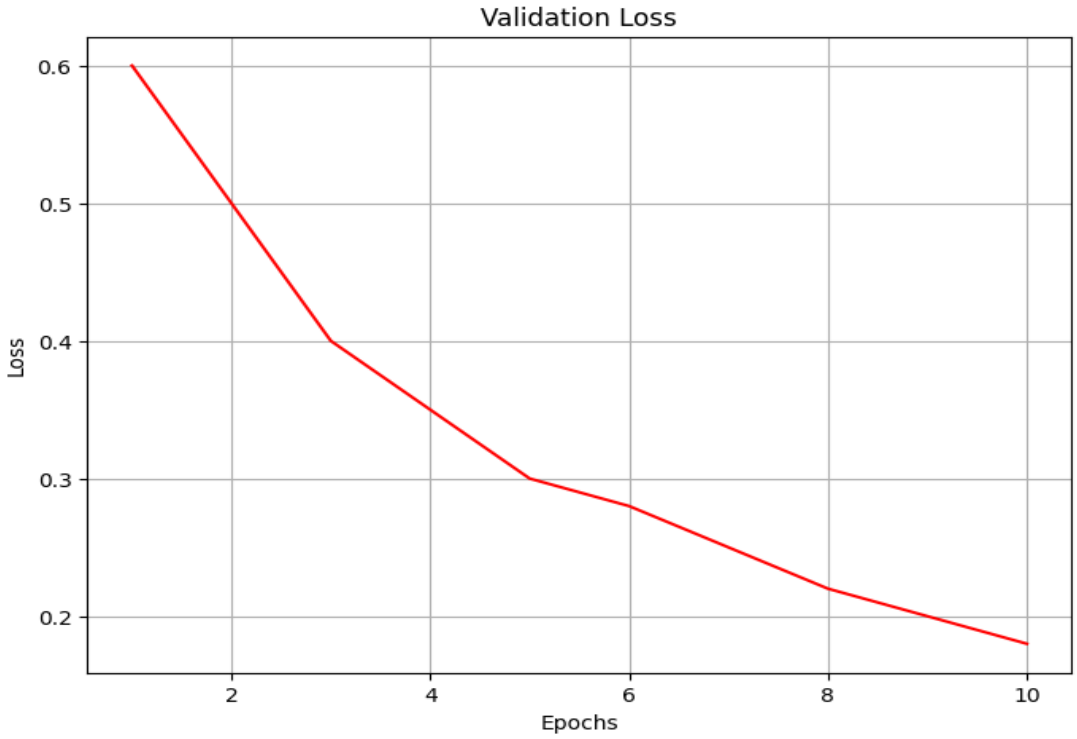

Fig. 14. Validation Loss of the Proposed Model

The performance of the proposed hybrid approach, which combines handcrafted features and CNN, the proposed method was compared with state-of-the-art techniques reported in recent studies. **Table 8** presents the performance comparison.

Table 8. Comparison of the Proposed Model with state-of-the-art Model

Ref	Method	Whole Tumor	Core Tumor	Active Tumor
[25]	Slice-wise 2D-patches extracted by 2D-CNN	0.83	0.73	0.69
[28]	3D-patches extracted by using 3D-CNN	0.86	0.74	0.71
[26]	Global and local 2D-patches with cascaded 2D-CNNs	0.86	0.79	0.73
[29]	Extract multi 2D patches using pixel level	0.67	Not reported	Not reported
[23]	2D-CNNs	0.76	0.81	0.73
Proposed System	**Handcrafted Features and Global Pathway**	**0.87**	**0.79**	**0.75**

The results show the overall GCNN performance is accurate. The results shown here are generated under the momentum of 0.9, weight decay of 0.1, the learning rate of 0.005, and stochastic gradient descent.

5. Conclusion

The existing methods for segmenting brain tumors primarily depend on manually designed characteristics (such as symmetry analysis, alignment-based feature analysis, or textural properties) or deep CNN. Handcrafted features aim to incorporate domain knowledge, while CNN approaches focus on unsupervised feature generation. Combining these methods in a cascaded manner has the potential to surpass the performance of other feature-based or data-driven techniques individually. The present study involved the development of a GCNN consist of CNN for CS Pathways to handle CS modalities in conjunction with the given ground truth, and another CNN for MRI Pathways. The objective of this study is to construct a proficient deep convolutional architecture supplemented with manually designed features capable of effectively managing various categories of tumors. This study highlights the potential of concatenating traditional feature-based approaches with deep learning methods to improve the accuracy of brain tumor segmentation. The proposed GCNN can be further refined and optimized to achieve even higher segmentation accuracy. Additionally, the approach can be extended to other medical imaging applications, such as the detection and segmentation of other types of tumors or lesions, to aid in diagnosis and treatment planning.

References

[1] R. Sullivan, O. I. Alatise, B. O. Anderson, R. Audisio, P. Autier, A. Aggarwal, C. Balch, M. F. Brennan, A. Dare, and A. D'Cruz, "Global cancer surgery: delivering safe, affordable, and timely cancer surgery," *The lancet oncology*, vol. 16, no. 11, pp. 1193-1224, 2015. Article (CrossRef Link)

[2] J. Liu, M. Li, J. Wang, F. Wu, T. Liu, and Y. Pan, "A survey of MRI-based brain tumor segmentation methods," *Tsinghua science and technology*, vol. 19, no. 6, pp. 578-595, 2014. Article (CrossRef Link)

[3] R. L. Kumar, J. Kakarla, B. V. Isunuri, and M. Singh, "Multi-class brain tumor classification using residual network and global average pooling," *Multimedia Tools and Applications*, vol. 80, pp. 13429-13438, 2021. Article (CrossRef Link)
[4] N. Zahid, W. Khalid, K. Ahmad, S. S. Bhamani, I. Azam, N. Asad, A. A. Jabbar, M. Khan, and A. Enam, "Resilience and quality of life (QoL) of head and neck cancer and brain tumour survivors in Pakistan: an analytical cross-sectional study protocol," *BMJ open*, vol. 9, no. 9, pp. e029084, 2019. Article (CrossRef Link)
[5] J. S. Lee, "A review of deep-learning-based approaches for attenuation correction in positron emission tomography," *IEEE Transactions on Radiation and Plasma Medical Sciences*, vol. 5, no. 2, pp. 160-184, 2021. Article (CrossRef Link)
[6] E. E. M. Azhari, M. M. M. Hatta, Z. Z. Htike, and S. L. Win, "Tumor detection in medical imaging: a survey," *International Journal of Advanced Information Technology*, vol. 4, no. 1, pp. 21-29, 2014. Article (CrossRef Link)
[7] S. Roy, and S. K. Bandyopadhyay, "Detection and Quantification of Brain Tumor from MRI of Brain and it's Symmetric Analysis," *International Journal of Information and Communication Technology Research*, vol. 2, no. 6, pp. 477-483, 2012. Article (CrossRef Link)
[8] S. Bauer, L. P. Nolte, and M. Reyes, "Fully automatic segmentation of brain tumor images using support vector machine classification in combination with hierarchical conditional random field regularization," in *Proc. of International Conference on Medical Image Computing and Computer-Assisted Intervention*, pp. 354-361, 2011. Article (CrossRef Link)
[9] L. Lüdemann, C. Warmuth, M. Plotkin, A. Förschler, M. Gutberlet, P. Wust, and H. Amthauer, "Brain tumor perfusion: Comparison of dynamic contrast enhanced magnetic resonance imaging using T1, T2, and T2* contrast, pulsed arterial spin labeling, and H215O positron emission tomography," *European journal of radiology*, vol. 70, no. 3, pp. 465-474, 2009. Article (CrossRef Link)
[10] W. Zhang, J. Pang, K. Chen, and C. C. Loy, "K-net: Towards unified image segmentation," *Advances in Neural Information Processing Systems*, vol. 34, pp. 10326-10338, 2021. Article (CrossRef Link)
[11] S. Hicks, D. Jha, V. Thambawita, P. Halvorsen, B.-J. Singstad, S. Gaur, K. Pettersen, M. Goodwin, S. Parasa, and T. de Lange, "Medai: Transparency in medical image segmentation," *Nordic Machine Intelligence*, vol. 1, no. 1, pp. 1-4, 2021. Article (CrossRef Link)
[12] F. Ullah, A. Salam, M. Abrar, and F. Amin, "Brain Tumor Segmentation Using a Patch-Based Convolutional Neural Network: A Big Data Analysis Approach," *Mathematics*, vol. 11, no. 7, pp. 1635, 2023. Article (CrossRef Link)
[13] M. H. Hasan, H. S. Hasan, and A. M. Hasan, "MRI Brain Scans Classification Using Bi-directional Modified Gray Level Co-occurrence Matrix and Long Short-Term Memory," *NeuroQuantology*, vol. 18, no. 9, pp. 54-63, 2020. Article (CrossRef Link)
[14] P. John, "Brain tumor classification using wavelet and texture based neural network," *International Journal of Scientific & Engineering Research*, vol. 3, no. 10, pp. 1-7, 2012. Article (CrossRef Link)
[15] G. Wang, W. Li, S. Ourselin, and T. Vercauteren, "Automatic brain tumor segmentation based on cascaded convolutional neural networks with uncertainty estimation," *Frontiers in computational neuroscience*, vol. 13, pp. 56, 2019. Article (CrossRef Link)
[16] S. J. S. Gardezi, and I. Faye, "Fusion of completed local binary pattern features with curvelet features for mammogram classification," *Applied Mathematics & Information Sciences*, vol. 9, no. 6, pp. 1-12, 2015. Article (CrossRef Link)
[17] Y. Xu, L. Lin, H. Hu, D. Wang, W. Zhu, J. Wang, X.-H. Han, and Y.-W. Chen, "Texture-specific bag of visual words model and spatial cone matching-based method for the retrieval of focal liver lesions using multiphase contrast-enhanced CT images," *International journal of computer assisted radiology and surgery*, vol. 13, pp. 151-164, 2018. Article (CrossRef Link)
[18] J. Cheng, W. Yang, M. Huang, W. Huang, J. Jiang, Y. Zhou, R. Yang, J. Zhao, Y. Feng, and Q. Feng, "Retrieval of brain tumors by adaptive spatial pooling and fisher vector representation," *PloS one*, vol. 11, no. 6, pp. 1-15, 2016. Article (CrossRef Link)

[19] B. H. Menze, A. Jakab, S. Bauer, J. Kalpathy-Cramer, K. Farahani, J. Kirby, Y. Burren, N. Porz, J. Slotboom, and R. Wiest, "The multimodal brain tumor image segmentation benchmark (BRATS)," *IEEE transactions on medical imaging*, vol. 34, no. 10, pp. 1993-2024, 2015. Article (CrossRef Link)

[20] Z. Xu, "Construction of Intelligent Recognition and Learning Education Platform of National Music Genre under Deep Learning," *Frontiers in Psychology*, vol. 13, 2022. Article (CrossRef Link)

[21] M. Bansal, M. Kumar, and M. Kumar, "2D object recognition techniques: state-of-the-art work," *Archives of Computational Methods in Engineering*, vol. 28, pp. 1147-1161, 2021. Article (CrossRef Link)

[22] F. Milletari, S. A. Ahmadi, C. Kroll, A. Plate, V. Rozanski, J. Maiostre, J. Levin, O. Dietrich, B. Ertl-Wagner, and K. Bötzel, "Hough-CNN: Deep learning for segmentation of deep brain regions in MRI and ultrasound," *Computer Vision and Image Understanding*, vol. 164, pp. 92-102, 2017. Article (CrossRef Link)

[23] H. Khan, P. M. Shah, M. A. Shah, S. ul Islam, and J. J. Rodrigues, "Cascading handcrafted features and Convolutional Neural Network for IoT-enabled brain tumor segmentation," *Computer communications*, vol. 153, pp. 196-207, 2020. Article (CrossRef Link)

[24] J. Kleesiek, A. Biller, G. Urban, U. Kothe, M. Bendszus, and F. Hamprecht, "Ilastik for multi-modal brain tumor segmentation," *Proceedings MICCAI BraTS (brain tumor segmentation challenge)*, vol. 12, pp. 17, 2014. Article (CrossRef Link)

[25] D. Zikic, Y. Ioannou, M. Brown, and A. Criminisi, "Segmentation of brain tumor tissues with convolutional neural networks," *Proceedings MICCAI-BRATS*, vol. 36, no. 2014, pp. 36-39, 2014. Article (CrossRef Link)

[26] M. Havaei, A. Davy, D. Warde-Farley, A. Biard, A. Courville, Y. Bengio, C. Pal, P.-M. Jodoin, and H. Larochelle, "Brain tumor segmentation with deep neural networks," *Medical image analysis*, vol. 35, pp. 18-31, 2017. Article (CrossRef Link)

[27] X. Liu, S. Hou, S. Liu, W. Ding, and Y. Zhang, "Attention-based Multimodal Glioma Segmentation with Multi-attention Layers for Small-intensity Dissimilarity," *Journal of King Saud University-Computer and Information Sciences*, vol. 35, no. 4, pp. 183-195, 2023. Article (CrossRef Link)

[28] B. Kayalibay, G. Jensen, and P. van der Smagt, "CNN-based segmentation of medical imaging data," *arXiv preprint arXiv:1701.03056*, 2017. Article (CrossRef Link)

[29] S. Iqbal, M. U. Ghani, T. Saba, and A. Rehman, "Brain tumor segmentation in multi-spectral MRI using convolutional neural networks (CNN)," *Microscopy research and technique*, vol. 81, no. 4, pp. 419-427, 2018. Article (CrossRef Link)

[30] "Multimodal Brain Tumor Segmentation Challenge 2018," [Online]. Available: https://www.med.upenn.edu/sbia/brats2018/data.html , Accessed on 9 February 2023

[31] S. Bagyaraj, R. Tamilselvi, P. B. Mohamed Gani, and D. Sabarinathan, "Brain tumour cell segmentation and detection using deep learning networks," *IET Image Processing*, vol. 15, no. 10, pp. 2363-2371, 2021. Article (CrossRef Link)

Faizan Ullah is currently pursuing the Ph.D. degree in computer science from International Islamic University Islamabad. His research interests include data mining, machine learning, and deep learning.

Dr MUHAMMAD NADEEM received Ph.D. degree from Department of Computer Science & Software Engineering International Islamic University. He is currently working as an Assistant Professor with the Department of Computer Science & Software Engineering International Islamic University. His research interests include bioinformatics, Medical Image Processing, Machine Learning & Computational Intelligence.

Dr. Mohammad Abrar is a distinguished researcher in the field of computer science, specializing in artificial intelligence, neural networks, classification, and federated learning. He earned his Ph.D. in computer science in 2013 from the prestigious University Technology Malaysia. With a keen interest in cutting-edge technologies, Dr. Abrar has made remarkable contributions to the field of AI. His expertise lies in the development and application of neural networks, specifically in classification. His research work has been published in reputable conferences and high-impact research journals, making a significant impact on the scientific community. Dr. Abrar's dedication and expertise in federated learning have paved the way for advancements in distributed machine learning algorithms, ensuring privacy-preserving and efficient training processes across decentralized data sources. His research findings have practical implications for various domains, including healthcare, finance, and telecommunications.